2016 IEEE 55th Conference on Decision and Control (CDC)
ARIA Resort & Casino
December 12-14, 2016, Las Vegas, USA

Decentralized Optimal Frequency Control of Interconnected Power Systems with Transient Constraints

Zhaojian Wang, Feng Liu, Steven H. Low, Changhong Zhao, Shengwei Mei

***Abstract*— We design decentralized frequency control of multi-area power systems that will re-balance power and drive frequencies to their nominal values after a disturbance. Both generators and controllable loads are utilized to achieve frequency stability while minimizing regulation cost. In contrast to recent results, the design is completely decentralized and does not require communication between areas. Our control enforces operational constraints not only in equilibrium but also during transient. Moreover, our control is capable of adapting to unknown load disturbance. We show that the closed-loop system is asymptotically stable and converges to an equilibrium that minimizes the regulation cost. We present simulation results to demonstrate the effectiveness of our design.**

I. Introduction

In a modern power system, multiple regional power grids are usually interconnected for improving operation reliability and economic efficiency. This paper addresses the decentralized optimal frequency control for restoring frequencies and tie-line power flows of such a system with transient operational constraints.

In the literature, different distributed strategies have been developed and applied to power system frequency control, which are mainly divided into two typical categories in terms of different regulation resources: the automatic generation control (AGC) [1], [2], [3] and the load-side frequency control [4], [5], [6], [7]. The former category focuses on the optimal regulation of generators. In [4] a flatness-based control combining trajectory generation and trajectory tracking is proposed for AGC in multi-area power systems. The trajectory generation is realized via economic dispatch globally, while the trajectory tracking is achieved by generation allocation based on PMU measurement. In [2], generators are driven by AGC to eliminate sudden frequency deviations. Correspondence between the partial primal-dual gradient algorithm for solving the associated optimization and the physical frequency control dynamics is established. The resulting decomposition method enables the design of fully distributed frequency control to solve the original centralized optimal frequency control problem.

As for the load-side frequency control, controllable load is utilized for frequency regulation. In [4], a distributed adaptive control to guarantee acceptable frequency deviation from the nominal value is presented. In [7], load frequency dynamics are formulated similar to the generator model, resulting in a distributed frequency control that takes both generation and controllable load into account. In [5], an optimal load control (OLC) problem is formulated, rendering an ubiquitous load-side primary frequency control based on the partial primal-dual gradient algorithm for solving the OLC problem. However, it does not restore the nominal frequency. To address this problem, [8] enforces a power balance constraint only on generation and frequency-insensitive load. [6] further proposes a distributed optimal load control, where the controllable load can individually estimate the power mismatch from frequency measurement. To mitigate the effects of measurement noise, communication between neighboring control areas is required.

In terms of design methodologies, distributed frequency control design mainly exhibits three trends: the droop control based approach [9], [10], the consensus based approach [11], [12], [13] and the primal-dual decomposition based approach [5], [14], [15]. [10] suggests a distributed adaptive droop controller for DC microgrid control with proportional load sharing. In [18], a theoretical framework for consensus based controller design is derived and several typical consensus controllers are provided. [13], [16] demonstrates that consensus can be achieved among PV generators with the same reserve ratio. Although the droop and the consensus based approaches lead to distributed control, the feasibility and optimality of controllers may not be guaranteed. The primal-dual decomposition based approach is associated with its specific centralized optimization counterpart whose solution is identical to the desired distributed controllers [14], [15]. Then typical primal-dual algorithms can be used to design the distributed optimal controllers [14]. However, this approach relies largely on specific properties of the associated optimization problem, such as convexity, which restricts its deployment. In practice, a control area always has certain regulation capacity bounds that restrict power generation and controllable load within an available range, either in equilibrium or during transient. Only steady-state constraints have been imposed in the literature. In contrast, we enforce constraints during transient as well. To do this, we design primal-dual based algorithms and prove that the closed-loop system remains asymptotically stable. Moreover, it converges to an optimal equilibrium point.

Specifically we reveal the correspondence between our controller and the primal-dual gradient algorithm for solving its optimization counterpart. Then we prove the optimality

This work was supported by the National Natural Science Foundation of China (No. 51321005, No. 51377092), Los Alamos National Lab through an DoE grant DE-AC52-06NA25396, and Skoltech through Collaboration Agreement 1075-MRA.

Z. Wang, F. Liu and S. Mei are with the Department of Electrical Engineering, Tsinghua University, Beijing, 10084, China lfeng@tsinghua.edu.cn

S. H. Low and C. Zhao are with the Department of Electrical Engineering, California Institute of Technology, Pasadena, CA, 91105 USA slow@caltech.edu

of our control by exploiting the equivalence between the equilibrium of the closed-loop system and the optimal solution of the optimization counterpart. We prove the stability of closed-loop system by combining projection technique with LaSalle invariant principle, excluding the impacts of nonsmooth dynamics created by the transient constraints. The salient features of our control are: 1) *Control goals:* it restores both nominal frequency and tie-line power after a disturbance while minimizing the regulation cost; 2) *Constraints:* regulation capacity constraints are enforced even during transient; 3) *Communication:* it is completely decentralized without the need for communication even among neighboring areas; 4) *Measurement:* our control is capable of adapting to unknown load disturbance autonomously with no requirement of load measurement.

The rest of this paper is organized as follows. In Section II, we formulate the optimal frequency control problem. Section III presents our controller and its relationship with the primal-dual update. We further prove the optimality and stability of the closed-loop system in Section IV. Then we confirm the performance of our controller in Section V. Section VI concludes the paper.

II. Problem formulation

A. Network model

A large power network is usually composed of multiple control areas each with its own generators and loads. These control areas are interconnected with each other through tie lines. For simplicity, we treat each control area as a node with an aggregate power generation, an aggregate controllable load and an aggregate uncontrollable load. Then the power network is model by a graph $G := (N,E)$ where $N = \{0,1,2,...n\}$ is the set of nodes (control areas) and $E \subseteq N \times N$ is the set of edges (tie lines). If a pair of nodes i and j are connected by a tie line directly, we denote the tie line by $(i,j) \in E$. Let $m := |E|$ denote the number of tie lines. Unless otherwise specified, graph G is considered undirected. Sometimes, however, we treat G as directed with an arbitrary orientation, in which case we use $(i,j) \in E$ or $i : i \to j$ interchangeably to denote the directed edge from i to j. It should be clear from the context which is the case. Without loss of generality, we assume the graph is connected and node 0 is a reference node (slack bus).

For each node $j \in N$ let $\theta_j(t)$ denote the rotor angle at node j at time t and $\omega_j(t)$ the frequency. Let $P_j^g(t)$ denote the (aggregate) generation at node j at time t and $u_j^g(t)$ its generation control command. Let $P_j^l(t)$ denote the (aggregate) controllable load and $u_j^l(t)$ its load control command. Let $p_j(t)$ denote the (aggregate) uncontrollable load.

We adopt a second-order linearized model to describe the frequency dynamics of each node, and two first-order inertia equations to describe the dynamics of power generation regulation and load regulation at each node. We assume the tie lines are lossless and adopt the DC power flow model.

Then for each node $j \in N$

$$\dot{\theta}_j = \omega_j(t) \tag{1a}$$

$$M_j\dot{\omega}_j = P_j^g(t) - P_j^l(t) - p_j - D_j\omega_j(t) + \sum_{i:i\to j} B_{ij}(\theta_i(t) - \theta_j(t)) - \sum_{k:j\to k} B_{jk}(\theta_j(t) - \theta_k(t)) \tag{1b}$$

$$T_j^g\dot{P}_j^g = -P_j^g(t) + u_j^g(t) - \frac{\omega_j(t)}{R_j} \tag{1c}$$

$$T_j^l\dot{P}_j^l = -P_j^l(t) + u_j^l(t) \tag{1d}$$

where $D_j > 0$ are damping constants, $R_j > 0$ are droop parameters, and $B_{jk} > 0$ are line parameters that depend on voltage magnitudes at nodes j,k and the reactance of the line (j,k). Let $x := (\theta, \omega, P^g, P^l)$ denote the state of the network and $u := (u^g, u^l)$ denote the control.[1]

Our goal is to design feedback control laws for the generation command $u^g(x(t))$ and load control $u^l(x(t))$. The operational constraints are:

$$\underline{P}_j^g \le P_j^g(t) \le \overline{P}_j^g, \quad j \in N \tag{2a}$$

$$\underline{P}_j^l \le P_j^l(t) \le \overline{P}_j^l, \quad j \in N \tag{2b}$$

We will design controllers so that these constraints are satisfied not only in equilibrium, but also during transient.

We assume that the system operates in a steady state initially, i.e., the generation and the load are balanced and the frequency is at its nominal value. All variables represent *deviations* from their nominal or scheduled values so that,e.g., $\omega_j(t) = 0$ means the frequency is at its nominal value.

There are two possible modes of operation. In the first mode, each node (control area) balances its own supply and demand after a disturbance. We design controls that will drive the power flow on each tie line to its scheduled value. In the second mode, all nodes cooperate to rebalance power over the entire network after a disturbance. The tie-lie power flows may deviate from their scheduled values and we require that they satisfy line limits. We refer to the first case as *per-node power balance* and the second *network power balance*.

Here we consider the per-node power balance case, modeled by the requirement:

$$P_j^g = P_j^l + p_j, \qquad j \in N \tag{3}$$

The network power balance case is modeled by the requirement:

$$\sum_j P_j^g = \sum_j \left(P_j^l + p_j\right) \tag{4}$$

instead of (3). This case is considered in the journal version of our paper.

[1]Given a collection of x_i for i in a certain set A, x denotes the vector $x := (x_i, i \in A)$ with x_i as its components.

B. Control goals

The control goals are formalized as:

$$\min \quad \frac{1}{2}\sum_j \alpha_j \left(P_j^g\right)^2 + \frac{1}{2}\sum_j \beta_j \left(P_j^l\right)^2 + \frac{1}{2}\sum_j D_j \omega_j^2 \tag{5a}$$

$$\text{over} \quad x := (\theta, \omega, P^g, P^l) \text{ and } u := (u^g, u^l)$$

$$\text{s. t.} \quad (2), (3)$$

$$P_j^g = P_j^l + p_j + E_j(\theta, \omega_j), \quad j \in N \tag{5b}$$

$$P_j^g = u_j^g, \quad j \in N \tag{5c}$$

$$P_j^l = u_j^l, \quad j \in N \tag{5d}$$

where $\alpha_j > 0$, $\beta_j > 0$ are constant weights and

$$E_j(\theta, \omega_j) := D_j \omega_j - \sum_{i:i\to j} B_{ij}\theta_{ij} + \sum_{k:j\to k} B_{jk}\theta_{jk}$$

Here we have abused notation and use $\theta_{ij} := \theta_i - \theta_j$. In vector form we have

$$E(\theta, \omega) := D\omega + CBC^T\theta \tag{6}$$

where $D := \mathrm{diag}(D_i, i \in N)$, $B := \mathrm{diag}(B_{ij}, (i,j) \in E)$, C is the $(n+1) \times m$ incidence matrix.

We comment on the optimization problem (5).

Remark 1 (Control goals)**.** 1) Since the variables are deviations from their nominal values, the parameters (α_j, β_j) in the objective function (5a) are not electricity costs. Minimizing the objective aims to track generation and consumption that have been scheduled at a slower timescale, e.g., to optimize economic efficiency or user utility. The parameters (α_j, β_j) weigh the relative costs of deviating from scheduled generation, load, and the nominal frequency.

2) For the definition of (5), the regulation capacity limits (2) apply only at optimality. The transient constraints can only be considered in the dynamic model.

3) The per-node balance requirement (3) and the constraint (5b) imply $E(\theta, \omega) = 0$ at any feasible x. This will drive the power flow on *every* line to its scheduled value (see Theorem 2 below). We assume that these scheduled values satisfy line limits and therefore do not impose line limits in (5).

4) The constraints (5c)(5d) require that, at optimality, the power injection P_j^g and controllable load P_j^l are equal to their control commands u_j^g and u_j^l respectively.

III. Controller design

A. Decentralized controllers

Our feedback control laws for u^g and u^l are: for each node $j \in N$

$$\dot{\lambda}_j = \gamma_j^\lambda \left(P_j^g(t) - P_j^l(t) - p_j\right) \tag{7a}$$

$$u_j^g(t) = \left[P_j^g(t) - \gamma_j^g\left(\alpha_j P_j^g(t) + \omega_j(t) + \lambda_j(t)\right)\right]_{\underline{P}_j^g}^{\overline{P}_j^g} + \frac{\omega_j(t)}{R_j} \tag{7b}$$

$$u_j^l(t) = \left[P_j^l(t) - \gamma_j^l\left(\beta_j P_j^l(t) - \omega_j(t) - \lambda_j(t)\right)\right]_{\underline{P}_j^l}^{\overline{P}_j^l} \tag{7c}$$

where $\gamma_j^m, \gamma_j^l, \gamma_j^\lambda$ are (strictly) positive constants. For any $x_i, a_i, b_i \in \mathbb{R}$ with $a_i \le b_i$, $[x_i]_{a_i}^{b_i} := \min\{b_i, \max\{a_i, x_i\}\}$. For vectors x, a, b, $[x]_a^b$ is defined accordingly componentwise.

The control is *completely decentralized* where each node j updates its *internal* state $\lambda_j(t)$ in (7a) based only on the generation $P_j^g(t)$, the controllable load $P_j^l(t)$ and the uncontrolled load $p_j(t)$ locally at j (within a control area). The control laws $u_j^g(t)$ and $u_j^l(t)$ in (7b) and (7c) are then static functions of the state $(P_j^g(t), P_j^l(t), \omega_j(t))$ and the internal state $\lambda_j(t)$. No communication is required between nodes.

We often write u_j^g and u_j^l as functions of $(P_j^g, P_j^l, \omega_j, \lambda_j)$: for $j \in N$

$$u_j^g(t) := u_j^g\left(P_j^g(t), \omega_j(t), \lambda_j(t)\right) \tag{8a}$$

$$u_j^l(t) := u_j^l\left(P_j^g(t), \omega_j(t), \lambda_j(t)\right) \tag{8b}$$

where these functions are given by the right-hand side of (7b) (7c). We now comment on measurements required to implement the control (7).

Remark 2 (Implementation)**.** The variable $\lambda_j(t)$ in (7a) is a cyber quantity that is computed at each node j based on the generation $P_j^g(t)$, the controllable load $P_j^l(t)$ and the uncontrolled load $p_j(t)$ locally at j (within a control area). These quantities can in principle be measured at j. We would however like to avoid measuring the uncontrolled load change $p_j(t)$ for the convenience in practice.

To this end, let $\Delta P_j(t) := P_j^g(t) - P_j^l(t) - p_j(t)$, $j \in N$, denote the surplus generation at node j. We then have from (1b) and (6) that $\Delta P_j(t) = M_j\dot{\omega}_j + E_j(\theta, \omega_j(t))$. Since $\dot{\lambda}_j = \gamma_j^\lambda \Delta P_j(t)$, (7a) becomes:

$$\dot{\lambda}_j = \gamma_j^\lambda M_j \dot{\omega}_j + \gamma_j^\lambda D_j \omega_j(t) - \gamma_j^\lambda\left(\sum_{i:i\to j} P_{ij}(t) - \sum_{k:j\to k} P_{jk}(t)\right)$$

where $P_{ij} := B_{ij}(\theta_i - \theta_j)$ are the tie-line flows from nodes i to j according to the DC power flow model. Hence, to update the internal state $\lambda_j(t)$, we only need to measure the local frequency deviation $\omega_j(t)$, its derivative $\dot{\omega}_j(t)$ and the tie-line flows $P_{ij}(t)$ incident on node j, and not the uncontrolled

load $p_j(t)$. A salient feature is that the controller naturally adapts to unknown load changes $p_j(t)$. This feature will be illustrated in case studies.

The control inputs $u_j^g(t)$ and $u_j^l(t)$ in (8) can then be implemented using measurements of the local generation $P_j^g(t)$, controlled load $P_j^l(t)$, frequency deviation $\omega_j(t)$ and the internal state $\lambda_j(t)$.

B. Design rationale

The controller design (7) is motivated by a partial primal-dual algorithm for (5) that dualizes the constraints (3) and (5b), as we now explain. Define the corresponding Lagrangian of (5) as:

$$\begin{aligned} L(x;\rho) &= \frac{1}{2}\sum_j \alpha_j \left(P_j^g\right)^2 + \frac{1}{2}\sum_j \beta_j \left(P_j^l\right)^2 + \frac{1}{2}\sum_j D_j\omega_j^2 \\ &\quad + \sum_j \lambda_j \left(P_j^g - P_j^l - p_j\right) \\ &\quad + \sum_j \mu_j \Big(P_j^g - P_j^l - p_j - D_j\omega_j \\ &\qquad + \sum_{i:i\to j} B_{ij}\theta_{ij} - \sum_{k:j\to k} B_{jk}\theta_{jk}\Big) \end{aligned} \tag{9}$$

where $\rho := (\lambda, \mu)$ are Lagrange multipliers of (5). A primal-dual algorithm takes the form

$$\dot{x} = -\Gamma_x \frac{\partial L}{\partial x}(x(t),\rho(t)) \tag{10a}$$

$$\dot{\rho} = \Gamma_\rho \frac{\partial L}{\partial \rho}(x(t),\rho(t)) \tag{10b}$$

where Γ_x, Γ_ρ are (strictly) positive diagonal gain matrices.

We will analyze the optimality and stability of the closed-loop system where the controls $u^g(x,\rho)$ and $u^l(x,\rho)$ are functions of (x,ρ) defined by the right-hand side of (7b)(7c). Hence the Lagrangian is defined to be only a function of (x,ρ) and does not involve $u := (u^g, u^l)$.

We now explain that *the closed-loop dynamics* (1)(7) *carries out an primal-dual algorithm* (10) *for solving* (5) *in real time over the power network.*

We first show that the control (7a) and the swing dynamic (1b) are carrying out the dual update (10b). We then show that the generation and load dynamic (1c) and (1d) are carrying out the primal update (10a). Finally we show that (1a) minimizes L over θ.

First the variable λ is the Lagrange multiplier vector for the per-node power balance constraint (3). It is a cyber quantity that the controllers update according to (7a). This control law is exactly the dual update (10b) in the primal-dual algorithm (in vector form):[2]

$$\dot{\lambda} = \Gamma^\lambda \nabla_\lambda L(x(t),\rho(t)) \tag{11a}$$

where $\Gamma^\lambda := \mathrm{diag}(\gamma_j^\lambda, j \in N)$.

[2]We use $\frac{\partial f}{\partial x}$ to denote a row vector and $\nabla_x f(x) := \left(\frac{\partial f}{\partial x}\right)^T$ a column vector.

Second the variable μ is the Lagrange multiplier vector for the constraint (5b). It can be identified with the frequency deviation ω because the KKT condition

$$\frac{\partial L}{\partial \omega_j}(x^*,\rho^*) = D_j(\omega_j^* - \mu_j^*) = 0$$

implies $\mu_j^* = \omega_j^*$ at optimality since $D_j > 0$. Moreover we can identify $\mu(t) \equiv \omega(t)$ during transient if we update the cyber quantity $\mu(t)$ according to

$$\begin{aligned} \dot{\mu} &= M^{-1}\left(P^g(t) - P^l(t) - p_j(t) - E(\theta(t),\omega(t))\right) \\ &= M^{-1}\,\nabla_\mu L(x(t),\rho(t)) \end{aligned} \tag{11b}$$

where $M := \mathrm{diag}(M_j, j \in N)$. Then μ and ω have the same dynamics (compared with (1b)) and hence $\mu(t) \equiv \omega(t)$ as long as $\mu(0) = \omega(0)$. Therefore the swing dynamic (1b) is equivalent to (11b) and carries out the dual update (10b) on the dual variable μ.

Third if we identify $\mu(t) \equiv \omega(t)$ then

$$\nabla_{P^g} L(x(t),\rho(t)) = A^g P^g(t) + \omega(t) + \lambda(t)$$

where $A^g := \mathrm{diag}(\alpha_j, j \in N)$. Therefore the control law (7b) is equivalent to

$$u^g(t) = [P^g(t) - \Gamma^g \nabla_{P^g} L(x(t),\rho(t))]_{\underline{P}^g}^{\overline{P}^g} + R^{-1}\omega(t)$$

where $\Gamma^g := \mathrm{diag}(\gamma_j^g, j \in N)$ and $R := \mathrm{diag}(R_j, j \in N)$. Then the generation dynamic (1c) becomes

$$\dot{P}^g = -P^g + [P^g(t) - \Gamma^g \nabla_{P^g} L(x(t),\rho(t))]_{\underline{P}^g}^{\overline{P}^g}$$

It can be verified that this is equivalent to

$$\dot{P}^g = [-\Gamma^g \nabla_{P^g} L(x(t),\rho(t))]_{-(P^g(t)-\underline{P}^g)}^{\overline{P}^g - P^g(t)} \tag{11c}$$

That is, the generator at each node j carries out the primal update (10a) with a saturation:

$$\dot{P}_j^g = \min\left\{\overline{P}_j^g - P_j^g(t),\ \max\left\{-\left(P_j^g(t) - \underline{P}_j^g\right),\ -\gamma_j^g \frac{\partial L}{\partial P_j^g}(x(t),\rho(t))\right\}\right\}$$

As shown in Lemma 3 below, the saturation in $u^g(t)$ ensures that $P^g(t)$ satisfies control capacity limits (2) at all times t.

Similarly the control law (7c) is equivalent to

$$u^l(t) = \left[P^l(t) - \Gamma^l \nabla_{P^l} L(x(t),\rho(t))\right]_{\underline{P}^l}^{\overline{P}^l}$$

where $\Gamma^l := \mathrm{diag}(\gamma_j^l, j \in N)$. The controllable load dynamic (1d) is equivalent to

$$\dot{P}^l = \left[-\Gamma^l\,\nabla_{P^l} L(x(t),\rho(t))\right]_{-(P^l(t)-\underline{P}^l)}^{\overline{P}^l - P^l(t)} \tag{11d}$$

i.e., the controllable load at each node j carries out the primal update (10a) with a saturation:

$$\dot{P}_j^l = \min\left\{\overline{P}_j^l - P_j^l(t),\ \max\left\{-\left(P_j^l(t) - \underline{P}_j^l\right),\ -\gamma_j^l \frac{\partial L}{\partial P_j^l}(x(t),\rho(t))\right\}\right\}$$

Finally, to relate (1a) to a primal update, note that the last term in the definition (9) of the Lagrangian L is:

$$\begin{aligned} &\sum_j \mu_j \left(\sum_{i:i\to j} B_{ij}\theta_{ij} - \sum_{k:j\to k} B_{jk}\theta_{jk} \right) \\ = \; & -\sum_{(i,j)\in E} B_{ij}(\mu_i-\mu_j)(\theta_i-\theta_j) \;=\; -\mu^T CBC^T\theta \end{aligned}$$

Hence in vector form

$$\begin{aligned} L \;=\; & \frac{1}{2}\left((P^g)^T A^g P^g + (P^l)^T A^l P^l + \omega^T D\omega\right) \\ & + \lambda^T\left(P^g - P^l - p\right) - \mu^T CBC^T\theta \end{aligned}$$

where $A^l := \mathrm{diag}(\beta_j, j\in N)$ and

$$\nabla_\theta L \;=\; -CBC^T\mu \;=\; -CBC^T\omega$$

This and (1a) imply

$$CBC^T\dot{\theta} \;=\; -\nabla_\theta L \tag{11e}$$

Crucially, this implication means that the physical dynamic (1a) implements a component of the primal-dual algorithm that minimizes L over θ. The converse is not necessarily true, i.e., (11e) does not imply (1) because CBC^T is an $(n+1)\times(n+1)$ matrix with rank n.

In summary the closed-loop system (1)(7) is almost equivalent to (11) in the sense that (1a) implies (11e), (1b) is equivalent to (11b), (1c) is equivalent to (11c), (1d) is equivalent to (11d), and (7a) is equivalent to (11a).

IV. Optimality and Stability

A. Optimality of equilibrium point

Given an $(x,\rho) := (\theta,\omega,P^g,P^l,\lambda,\mu)$, recall that the control input $u(x,\rho)$ is given by (8).

Definition 1. A point $(x^*,\rho^*) := (\theta^*,\omega^*,P^{g*},P^{l*},\lambda^*,\mu^*)$ is an *equilibrium point* or an *equilibrium* of the closed-loop system (1)(7) if

1) The right-hand side of (1) vanishes at x^* and $u(x^*,\rho^*)$.
2) The right-hand side of (7a) vanishes at x^*.

Definition 2. A point (x^*,ρ^*) is *primal-dual optimal* if $(x^*,u(x^*,\rho^*))$ is optimal for (5) and ρ^* is optimal for its dual problem.

Section III-B says that the closed-loop system (1)(7) carries out an primal-dual algorithm in real time to solve (5). In this section we prove that a point (x^*,ρ^*) is an equilibrium of the closed-loop system if and only if it is primal-dual optimal. Moreover the equilibrium is almost unique. In the next subsection we prove that the closed-loop dynamics converge to the equilibrium point. We make the following assumption:

A1: Problem (5) is feasible and has a finite optimal solution.

Then we have the following theorems

Theorem 1. Suppose assumption A1 holds. A point (x^*,ρ^*) is primal-dual optimal if and only if (x^*,ρ^*) is an equilibrium of the closed-loop system (1)(7) that satisfies (2) and $\mu^*=0$.

Theorem 2. Suppose assumption A1 holds. Let (x^*,ρ^*) be primal-dual optimal. Then

1) x^* and μ^* are unique, with θ^* being unique up to an (equilibrium) reference angle θ_0^*. For $j\in N$, λ_j^* is unique if either $\underline{P}_j^g < P_j^{g*} < \overline{P}_j^g$ or $\underline{P}_j^l < P_j^{l*} < \overline{P}_j^l$.
2) nominal frequencies are restored, i.e., $\omega_j^* = 0$ for all $j\in N$; moreover $\theta_j^* = \theta_0^*$ for all $j\in N$.
3) the power flow $P_{ij}^* := B_{ij}(\theta_i^*-\theta_j^*) = 0$ holds on every tie line $(i,j)\in E$.
4) If $\underline{P}_j^g < P_j^{g*} < \overline{P}_j^g$ and $\underline{P}_j^l < P_j^{l*} < \overline{P}_j^l$ then, at optimality, the marginal generation regulation cost is equal to the marginal load regulation cost at node j, i.e., $\alpha_j P_j^{g*} = -\beta_j P_j^{l*} = -\mu_j^*$.

Remark 3. 1) Theorem 1 shows the equivalence between the equilibrium of closed-loop system and the primal-dual optimal solution. It also implies that, in equilibrium, per-node power balance (3) is achieved and the operational constraints (2) are satisfied.
2) Theorem 2 says the equilibrium point is almost unique and has a very simple structure.

B. Asymptotic stability

Next we justify the asymptotic stability of the closed-loop system (1) (7).We start with the following assumption.

A2: The initial states, $u_j^g(0)$ and $u_j^l(0)$, of the closed-loop system (1)(7) strictly satisfy constraint (2).

Since (1c)(1d) and (7b)(7c) are first-order inertia dynamics, it is easy to prove that every trajectory starting from an initial state that satisfies the regulation capacity limits (2) will satisfy these capacity limits for all $t>0$.

Lemma 3. Suppose A2 holds. Then trajectories $P_j^g(t)$ and $P_j^l(t)$ of the closed-loop system (1)(7) satisfy constraint (2) for all $t>0$.

We now turn to the stability of the closed-loop system (1)(7). Inspired by [17], we use the projection operator to describe the saturation dynamics of the controller (7). Let $\|\cdot\|_G$ denote the G-norm defined in $\mathbb{R}^n$ by $\|\xi\|_G = \langle\xi, G\xi\rangle$ for $\xi\in\mathbb{R}^n$, where $\langle\cdot,\cdot\rangle$ is the inner product in $\mathbb{R}^n$ while G is an $n\times n$ symmetric positive matrix. Then the projection of a point $\xi\in\mathbb{R}^n$ onto a closed convex set S, denoted by $\mathrm{Proj}_{S,G}(\xi):\mathbb{R}^n\to S$ is defined as the (unique) solution of $\min_{y\in S}\|y-\xi\|_G$. The projection operator is non-expansive and for all $\xi\in\mathbb{R}^n$, $\mathrm{Proj}_{S,G}(\xi)$ satisfies

$$\langle \xi - \mathrm{Proj}(\xi)_{S,G},\; G(\chi - \mathrm{Proj}(\xi)_{S,G})\rangle \le 0, \quad \chi\in S \tag{12}$$

Let $\tilde{\theta}(t) := C^T\theta(t)$. The closed-loop system (1)(7) can be converted, in vector form, into

$$\dot{\tilde{\theta}}(t) = C^T\omega(t) \quad (13a)$$

$$\dot{\omega}(t) = M^{-1}\left(P^g(t) - P^l(t) - p - D\omega(t) - CB\tilde{\theta}(t)\right) \quad (13b)$$

$$\dot{P}^g(t) = (T^g)^{-1}\left(-P^g(t) + [u^g(t)]_{\underline{u}^g}^{\overline{u}^g}\right) \quad (13c)$$

$$\dot{P}^l(t) = (T^l)^{-1}\left(-P^l(t) + [u^l(t)]_{\underline{u}^l}^{\overline{u}^l}\right) \quad (13d)$$

$$\dot{\lambda}(t) = \Gamma^\lambda\left(P^g(t) - P^l(t) - p\right) \quad (13e)$$

where $T^g := \mathrm{diag}(T_j^g, j \in N)$; $T^l := \mathrm{diag}(T_j^l, j \in N)$.

Denote $z := (\tilde{\theta}, \omega, P^g, P^l, \lambda)$, and

$$F(z) = \begin{bmatrix} -\Gamma^{\tilde{\theta}} BC^T\omega(t) \\ -\Gamma^\omega\left(P^g(t) - P^l(t) - p - D\omega(t) - CB\tilde{\theta}(t)\right) \\ \Gamma^g\left(A^gP^g(t) + \omega(t) + \lambda(t)\right) \\ \Gamma^l\left(A^lP^l(t) - \omega(t) - \lambda(t)\right) \\ -\Gamma^\lambda\left(P^g(t) - P^l(t) - p\right) \end{bmatrix} \quad (14)$$

where $\Gamma^{\tilde{\theta}} := \mathrm{diag}(\sqrt{B_{ij}^{-1}}, (i,j) \in E)$; $\Gamma^\omega := \mathrm{diag}(\sqrt{M_j^{-1}}, j \in N)$; $\Gamma^g := \mathrm{diag}((T_j^g)^{-1}, j \in N)$; $\Gamma^l := \mathrm{diag}((T_j^l)^{-1}, j \in N)$; $\Gamma^\lambda := \mathrm{diag}(\gamma_j^\lambda, j \in N)$.

In terms of the definition above, we simply let $G = I$ and

$$S := \{(P^g, P^l) \mid \underline{P}^g \le P^g \le \overline{P}^g,\ \underline{P}^l \le P^l \le \overline{P}^l,\ j \in N\}$$

Since Lemma 3 indicates that $P^g(t)$ and $P^l(t)$ are always within S, we can define the projection of $z(t) - F(z(t))$ on to the closed convex set S as $H_I(z(t)) := \mathrm{Proj}_{S,I}(z(t) - F(z(t)))$. Then system (13) can be rewritten as

$$\dot{z}(t) = \Gamma(H_I(z(t)) - z(t)) \quad (15)$$

where $\Gamma = \mathrm{diag}(\Gamma^{\tilde{\theta}}, \Gamma^\omega, \Gamma^g, , \Gamma^l, \Gamma^\lambda)$.

Then we consider a Lyapnunov function candidate as

$$V_b(z(t)) = -\langle F(z(t)),\ H_I(z(t)) - z(t)\rangle - \frac{1}{2}||H_I(z(t)) - z(t)||_2^2 \quad (16)$$

Let z^* denote the equilibrium of (15) or (13). Then we have $H_I(z^*) = z^*$, implying $V_b(z^*) = 0$. In addition, in light of Theorem 3.1 in [17] , $V_b(z)$ is non-negative. Then in terms of (16), we have the following theorems.

Theorem 4. Suppose A1 and A2 hold. Then

1) Every trajectory $z(t)$ of (13) starting from a finite initial state asymptotically converges to its equilibrium $z^* \in Z_b^*$ as $t \to +\infty$, where $Z_b^* := \{z \mid \dot{z}(t) \equiv 0\}$;
2) Constraint (2) is satisfied for all $t > 0$.
3) At equilibrium, $\omega^* = \tilde{\theta}^* = 0$.

Theorem 5. Suppose A1 and A2 hold. Then

1) Closed-loop system (1)(7) asymptotically converges to its equilibrium (x^*, ρ^*) defined by Definition 1.
2) Constraint (2) is satisfied for all $t > 0$.

Remark 4. Theorem 4 and Theorem 5 indicate that the system (13) and the closed-loop system (1)(7) are *"globally"* stable, i.e., the two systems are asymptotically stable provided both the equilibrium point and the initial state are within the feasible region.

The proof of Theorem 4 relies on a lemma that characterizes the monotonic decreasing property of $V_b(t)$ subject to (13).

Lemma 6. Suppose A1 and A2 hold. Then $V_b(z)$ is always decreasing along system (13). Moreover, every trajectory $z(t)$ of (13) starting from a finite initial state ultimately converges to the largest positive invariant subset Z_b^* of $Z_b^+ := \{z \mid \dot{\omega} = \dot{P}^g = \dot{P}^l = 0\}$ as $t \to +\infty$.

Based on Lemma 6, we can further prove that Z_b^+ implies Z_b^*, thus completes the proof of Theorem 4.

As Theorem 4 confirms the asymptotic stability of (13), we only need to prove it is equivalent to the asymptotic stability of system (1)(7). It can be justified by the following lemma.

Lemma 7. Suppose assumptions A1 and A2 hold. Then the following are equivalent.

1) The system (13) is asymptotically stable at its equilibrium Z_b^*;
2) The closed-loop system (1)(7) is asymptotically stable at its equilibrium (x^*, ρ^*) defined by Definition 1.

Then Theorem 5 is a direct result of Theorem 4, Lemma 7, Theorem 1, Theorem 2 and Lemma 3.

V. Cast Studies

A. System configuration for test

We use a four-area IEEE 39-bus system with slight modifications [1] to test our decentralized optimal frequency controller (see Fig. 1). For better power balance in area 2, we remove the line between bus 1 and bus 39, move the load on bus 16 to bus 19. Then we set generators #2, #4, #6, #8 as frequency regulation units. The controllable loads are aggregated and directly add on the generator nodes. The parameters of generators and controlled loads are given in Table I. Other parameters can be found in [1] [18].

TABLE I:
System parameters

Area j	D_j	R_j	α_j	β_j	T_j^g	T_j^l
1	1.3	0.04	2.7	3.0	6.56	5.46
2	1.4	0.06	2.92	3.6	5.69	4.74
3	1.4	0.05	3.15	4.2	7.3	6.08
4	1.2	0.045	3.38	4.8	6.7	5.58

In the simulation, we add step changes on the loads of all four areas to test the performance of our controller. The load changes are given in Table II, which are unknown to the decentralized controllers. We also show the operational constraints on generations and controllable loads in individual control areas in Table II.

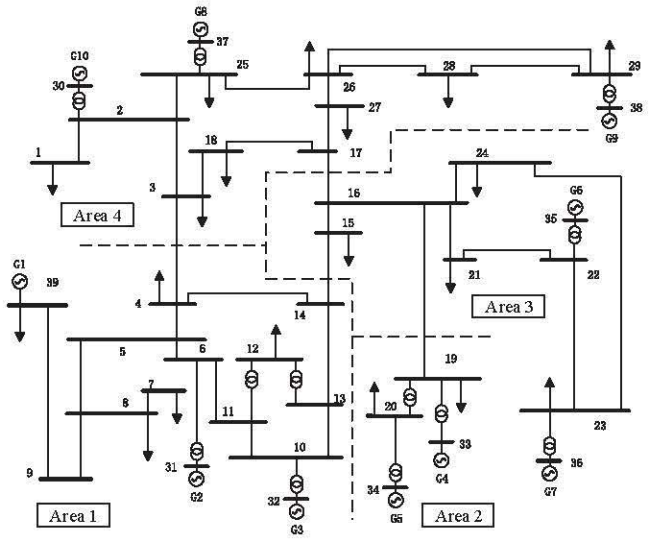

Fig. 1: IEEE 4-area, 39-bus system

TABLE II:
CAPACITY LIMITS AND LOAD DISTURBANCE

Area j	Load changes	$[\underline{P}_j^g, \overline{P}_j^g]$ (p.u.)	$[\underline{P}_j^l, \overline{P}_j^l]$ (p.u.)
1	0.1	[-0.07, 0.07]	[-0.07, 0.07]
2	0.15	[-0.105, 0.105]	[-0.105, 0.105]
3	-0.075	[-0.0525, 0.0525]	[-0.0525, 0.0525]
4	0.125	[-0.0875, 0.0875]	[-0.0875, 0.0875]

B. Stability and optimality

The dynamics of local frequencies and tie-line power flows are illustrated in Fig.2, where the left is the frequency dynamics, and the right is the tie-line power dynamics. Both the frequency and tie-line power deviations are restored in all four control areas. The generation and controllable load are different from that before the disturbance, indicating that the system is stabilized at a new equilibrium point. The new equilibrium point is given in Table III, which is identical to the optimal solution of (5) by using centralized optimization. These simulation results confirm that our controller can autonomously guarantee frequency stability while achieving optimal operating point in a fully decentralized manner.

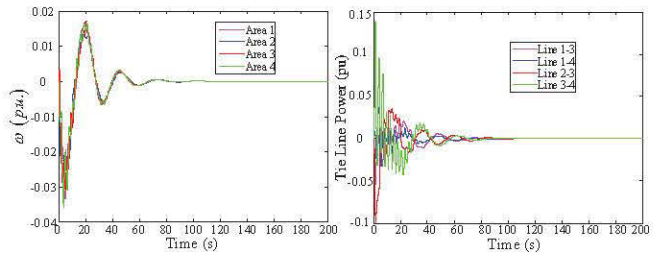

Fig. 2: Dynamics of frequency and tie-line flows

C. Dynamic property

In this subsection, we analyze the impacts of operational (capacity) constraints on the dynamic property. To do this,

TABLE III:
EQUILIBRIUM POINTS

	Area 1	Area 2	Area 3	Area 4
P_j^{g*}	0.0526	0.0828	-0.0429	0.0734
P_j^{l*}	0.0474	0.0672	-0.0321	0.0516

we compare the dynamic response of the frequency controllers with and without input saturation. The trajectories of generators' outputs and controllable loads are shown in Fig.3 and Fig.4, respectively. We found in both cases, the system frequency and tie-line flows are restored, and the same optimal equilibrium point is achieved. With input saturation, the trajectories of both generation and controllable load remain within their capacity limits even during transient. Without input saturation, however, capacity constraints are frequently violated during transient.

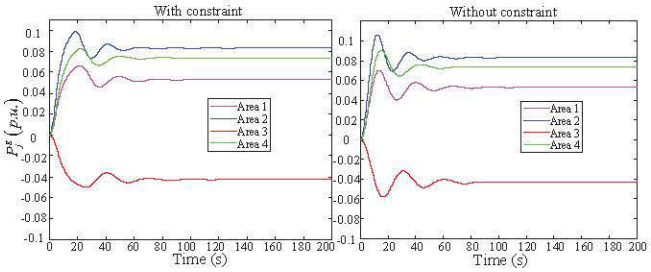

Fig. 3: Generators' outputs with/without capacity constraints

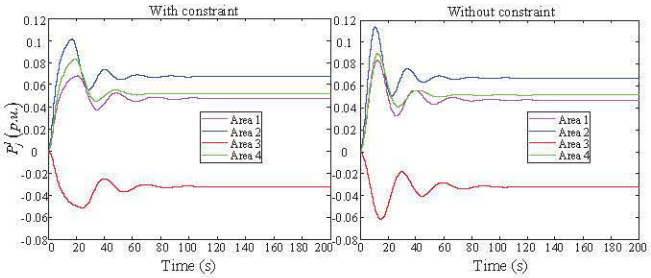

Fig. 4: Controllable loads with/without capacity constraints

D. Adaptation to unknown load change

In this subsection, we add 0.05p.u. load in area 2 at 100s, while keeping other conditions unchanged. The load change is unknown to individual control areas. Then each control area estimates the regional power difference using the method suggested in Remark 2. The power generation and controllable load dynamics are illustrated in Fig.5. Both generation and controllable load in control area 2 increase rapidly to rebalance power within the area, while other areas remain almost unchanged. The new equilibrium is close to the optimal solution given by centralized optimization (5). This result indicates that our controller is capable of correctly distinguishing between inside or outside disturbance and then adaptively compensating it even if it is unknown.

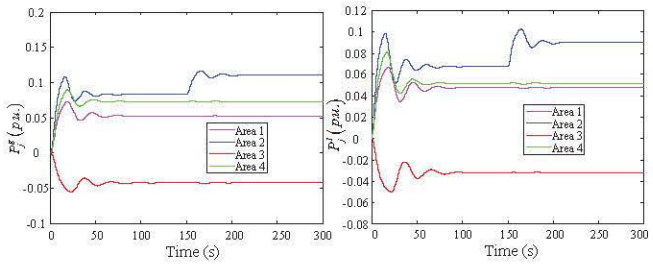

Fig. 5: Dynamic response to unknown load change

VI. Conclusion and Future Research

We have studied the decentralized frequency control of individual control areas with aggregate generators and controllable loads. Our controller can autonomously restore both the frequency and tie-line power after unknown load disturbance while minimizing the regulation cost. The operational constraints can be satisfied even in transient. Our controller is completely decentralized without the need for communication between control areas. We have revealed that the closed-loop system carries out an primal-dual algorithm to solve the associated optimal dispatch problem, hence guarantees the optimality of closed-loop equilibrium point. Although conventional stability analysis based on primal-dual theory does not apply due to the embedded saturation of the controller, we have alternatively used the projection technique to prove the stability of the closed-loop system. Simulations on the IEEE 39-bus power system verifies our theoretic results.

In this work, we do not consider the cooperation among control areas, where the tie-line powers are not fixed, but bounded within given ranges. Our ongoing work shows that this can be achieved via a distributed control. A crucial implication is it may provide a systematic way to bridge the gap between the (secondary) frequency control in a fast timescale and the economic dispatch in a slow timescale.

References

[1] M. H. Variani and K. Tomsovic, "Distributed automatic generation control using flatness-based approach for high penetration of wind generation," *IEEE Trans. Power Syst.*, vol. 28, no. 3, pp. 3002–3009, Apr. 2013.

[2] N. Li, L. Chen, C. Zhao, and S. H. Low, "Connecting automatic generation control and economic dispatch from an optimization view," in *Proc. American Control Conference (ACC)*, Portland, OR, Jun. 2014, pp. 735–740.

[3] I. Ibraheem, P. Kumar, and D. P. Kothari, "Recent philosophies of automatic generation control strategies in power systems," *IEEE Trans. Power Syst.*, vol. 20, no. 1, pp. 346–357, Feb. 2005.

[4] M. Zribi, M. Al-Rashed, and M. Alrifai, "Adaptive decentralized load frequency control of multi-area power systems," *International Journal of Electrical Power & Energy Systems*, vol. 27, no. 8, pp. 575–583, Oct. 2013.

[5] C. Zhao, U. Topcu, N. Li, and S. H.Low., "Design and stability of load-side primary frequency control in power systems," *IEEE Trans. Autom. Control*, vol. 59, no. 5, pp. 1177–1189, Jan. 2014.

[6] C. Zhao, U. Topcu, and S. H. Low, "Optimal load control via frequency measurement and neighborhood area communication," *IEEE Trans. Power Syst.*, vol. 28, no. 4, pp. 3576–3587, Nov 2013.

[7] M. D. Ilic, L. Xie, U. A. Khan, and J. M. F. Moura, "Modeling of future cyber-physical energy systems for distributed sensing and control," *IEEE Trans. Systems, Man, Cybern. A, Syst. Hum*, vol. 40, no. 4, pp. 825–838, July 2010.

[8] E. Mallada and S. H. Low, "Distributed frequency-preserving optimal load control," in *IFAC World congress*, 2014, pp. 5411–5418.

[9] A. Maknouninejad, Z. Qu, F. L. Lewis, and A. Davoudi, "Optimal, nonlinear, and distributed designs of droop controls for dc microgrids," *IEEE Trans. Smart Grid*, vol. 5, no. 5, pp. 2508–2516, Sept 2014.

[10] V. Nasirian, A. Davoudi, F. L. Lewis, and J. M. Guerrero, "Distributed adaptive droop control for dc distribution systems," *IEEE Trans. Energy Convers*, vol. 29, no. 4, pp. 944–956, Dec 2014.

[11] P. Yi, Y. Hong, and F. Liu, "Distributed gradient algorithm for constrained optimization with application to load sharing in power systems," *Systems & Control Letters*, vol. 83, pp. 45–52, Sept 2015.

[12] G. Binetti, A. Davoudi, F. L. Lewis, D. Naso, and B. Turchiano, "Distributed consensus-based economic dispatch with transmission losses," *IEEE Trans. Power Syst.*, vol. 29, no. 4, pp. 1711–1720, 2014.

[13] H. Xin, Z. Lu, Y. Liu, and D. Gan, "A center-free control strategy for the coordination of multiple photovoltaic generators," *IEEE Trans. Smart Grid*, vol. 5, no. 3, pp. 1262–1269, May 2014.

[14] C. Zhao and S. H. Low, "Decentralized primary frequency control in power networks," *arXiv*, vol. abs/1403.6046, 2014.

[15] N. Chen, L. Gan, S. H. Low, and A. Wierman, "Distributional analysis for model predictive deferrable load control," in *Decision and Control (CDC), 2014 IEEE 53rd Annual Conference on*, Los Angeles, CA, Dec 2014, pp. 6433–6438.

[16] H. Xin, Z. Lu, Z. Qu, D. Gan, and D. Qi, "Cooperative control strategy for multiple photovoltaic generators in distribution networks," *IET Control Theory Applicat*, vol. 5, no. 14, pp. 1617–1629, Sept 2011.

[17] M. Fukushima, "Equivalent differentiable optimization problems and descent methods for asymmetric variational inequality problems," *Math. programming*, vol. 53, no. 1-3, pp. 99–110, Jan 1992.

[18] T. Athay, R. Podmore, and S. Virmani, "A practical method for the direct analysis of transient stability," *IEEE Trans. Power Apparat. Syst.*, vol. PAS-98, no. 2, pp. 573–584, March 1979.